Archaeological and Anthropological Sciences (2026) 18:141
https://doi.org/10.1007/s12520-026-02499-1

RESEARCH

Reconstructing human–animal interactions via multiproxy analysis of dog paleofeces from the medieval Central Balkans

Nemanja Marković[1] · Freya Steinhagen[2,3] · Elena Marinova[3,4] · Samantha Brown[3,5] · Susan M. Mentzer[2,3] · Christopher E. Miller[2,3] · Maria A. Spyrou[2,3] · Víctor Roces[6] · Ella Reiter[3] · Dejan Bulić[7] · Mirjana Roksandić[8] · Piers D. Mitchell[9] · Cosimo Posth[2,3]

Received: 20 December 2025 / Accepted: 29 April 2026

Abstract

In archaeology, far more research has been performed on paleofeces of ancient humans than their companion animals, for which little is known. This study presents a multiproxy analysis of a paleofeces of dog origin, recovered from the medieval fortification of Gradina-Radaljevo (Serbia). The specimen was first recorded non-invasively through stereomicroscopy and micro-computed tomography, which documented a compact, flat-conical morphology containing highly digested bone fragments, charcoal, and sediment inclusions, features typical of carnivore digestion. Subsequent petrographic thin-sectioning and µFTIR confirmed a hydroxylapatite-rich matrix with cancellous and compact bone fragments, plant remains, and vegetal voids corresponding to cereal husk imprints, suggesting dietary ingestion of both animal and plant material. Paleoparasitological screening identified 26 helminth eggs belonging to *Ascaris* sp., *Trichuris* sp., and *Dicrocoelium* sp. Their morphology and low abundance indicate passive passage via ingestion of contaminated food, herbivore dung, or human waste rather than true infection of the host. Palynological analysis revealed low pollen diversity dominated by Poaceae, Cyperaceae, and fern spores, alongside wetland NPPs and *Glomus* fungi, reflecting environmental ingestion and scavenging behaviors. ZooMS of ingested bone fragments identified Suidae and Gallus, while aDNA analysis recovered Suidae, Bovidae, Phasianidae, and Canidae, including *Canis lupus familiaris*, further supporting a dog origin for the specimen. Together, these results indicate an omnivorous scavenging dog living near the settlement, consuming household refuse and fecal material, thereby mirroring human–animal interaction, sanitation practices, and parasite circulation in medieval Europe. This study sheds light on the complexity of human, dog and herbivore coexistence, contributing to the understanding of hygienic and sanitary conditions in medieval Europe.

Keywords Coprolite · Thin section · Paleoparasitology · Palynology · ZooMS · ADNA

✉ Nemanja Marković
nemamarkovic@gmail.com

[1] Institute of Archaeology, Knez Mihailova 35/IV, 11000 Belgrade, Serbia

[2] Senckenberg Centre for Human Evolution and Palaeoenvironment, University of Tübingen, Tübingen, Germany

[3] Institute for Archaeological Sciences, Department of Geosciences, University of Tübingen, Hölderlinstr 12, 72074 Tübingen, Germany

[4] Laboratory for Archaeobotany, Baden-Württemberg State Office for Cultural Heritage, Fischersteig 9, 78343 Hemmenhofen, Germany

[5] National Research Center On Human Evolution (CENIEH), 09002 Burgos, Spain

[6] Department of Molecular Biology, Max Planck Institute for Biology in Tübingen, Max-Planck-Ring 5, 72076 Tübingen, Germany

[7] The Institute of History Belgrade, Knez Mihailova 36/II, 11000 Belgrade, Serbia

[8] Department of Anthropology, University of Winnipeg, 515 Portage Avenue, Winnipeg, MB R3B 2E9, Canada

[9] Department of Archaeology, The McDonald Institute for Archaeological Research, University of Cambridge, Downing Street, Cambridge CB2 3ER, UK

Published online: 19 May 2026

Introduction

Ancient feces, also known as paleofeces or coprolites, serve as unique records that capture short-term evidence of an individual organism's diet and environmental context, providing valuable insights for paleoecological, paleontological, and archaeological research. These materials encapsulate a wealth of biological and environmental information, offering direct access to aspects of an individual life such as diet, health, parasitic infections, gut microbiota, and ecological relationships. The scientific value of human paleofeces has gained increasing recognition in recent years, especially as multidisciplinary strategies incorporating macrofossil, microscopic, and biomolecular analyses become more prevalent. These comprehensive approaches are particularly effective in investigating historical parasitic infections, which are essential markers of health status, sanitation, lifestyle, and environmental exposure in past populations (Barbera and Reinhard 2024; Blong and Shillito 2021; Blong et al. 2023; Reinhard et al. 1986; 2019).

Core analytical techniques—like pollen, and parasite egg analysis—continue to underpin paleofeces research. Yet these are now often complemented by advanced methodologies, including ancient DNA (aDNA) sequencing, lipid biomarker detection, stable isotope profiling, and scanning electron microscopy (Reinhard et al. 2019; Shillito et al. 2020a; 2020b). When used together, these techniques improve the ability to identify parasite species, assess their prevalence, and examine their ecological and cultural associations with human hosts. Recent studies highlight the potential of metagenomic analyses on paleofeces to classify host species and diet reconstruction in historic and prehistoric contexts (Blong and Shillito 2021; Ledger et al. 2019a; 2025; Witt et al. 2021).

Paleofeces research benefits from cross-disciplinary integration of parasitology, ecology, cultural, and molecular evidence, providing minimally invasive insights into past health and behavior. However, destructive analyses pose ethical challenges, as current guidelines focus on pre-sampling and offer limited guidance for responsibly conducting invasive procedures on these rare and valuable specimens (Blong and Shillito 2021; Blong et al. 2023).

In response to both methodological and ethical challenges, researchers have increasingly adopted multiproxy approaches that maximize data recovery while minimizing specimen loss. Although such analyses, integrating diverse lines of evidence from paleofeces, are becoming more common, they are not yet standard practice (Ledger et al. 2019a; Tolar et al. 2021). In this study, we apply a multiproxy workflow with particular emphasis on parasitic remains to enhance understanding of historical health patterns and human–pathogen–environment interactions, while preserving material for future research.

In cases where direct evidence from human remains is absent or limited, animals living in close association with people can provide a meaningful proxy for reconstructing aspects of human diet and health. Among these, dogs are especially informative due to their shared habitats, overlapping diets, and susceptibility to similar parasites. Moreover, the preservation of parasites or pathogenic microbes in canine paleofeces opens an additional window onto the health conditions of the humans who interacted with them (Ledger et al. 2019b; Maicher et al. 2021; Mitchell et al. 2022; Slepchenko et al. 2025a; Witt et al. 2021). We analyzed a likely dog paleofeces from a medieval household in Serbia to better understand how dogs dealt with human-related waste.

Materials and methods

Archaeological background

The supposedly dog paleofeces analyzed in this study was recovered during systematic archaeological excavations carried out in 2017 at the Upper Town Plateau of the medieval fortress site of Gradina-Radaljevo. The site is situated in the village of Radaljevo, approximately 10 km north of Ivanjica, in southwestern Serbia (Fig. 1a–b). Archaeological investigations at Gradina-Radaljevo were conducted in two phases, first between 2006–2008 and later from 2016–2018. Based on ceramic assemblages, rampart construction techniques, and architectural features of the towers, the most intensive phase of fortification is attributed to the second half of the fourteenth century (Marković et al. 2023).

During excavation, the Upper Town Plateau was divided by a one-meter-wide north–south control profile to document vertical stratigraphy. The uppermost layer consisted of light brown humus with roots, abundant stones (including ashlars and siga fragments) and finds such as pottery, animal bones, a broken stone whetstone, and a small iron coin. Beneath this, a rubble deposit of stones, mortar fragments, and ashlars contained numerous animal bones, pottery sherds, iron coins, and carved stone fragments along the southern rampart. Below the rubble, a thin yellow–brown soil layer with scattered finds suggested fire exposure. In the southern sector, additional rubble and dark brown soil with cinders, charred wood, whitewash fragments, and small stones indicated concentrated fire activity, producing abundant pottery, bones, and occasional metal objects. This entire area is interpreted as a single midden. In the western half near the southern rampart, a paleofeces specimen was recovered, dated to the late 13th–fourteenth century based on stratigraphy and associated pottery. The chronology is more precisely constrained to the second

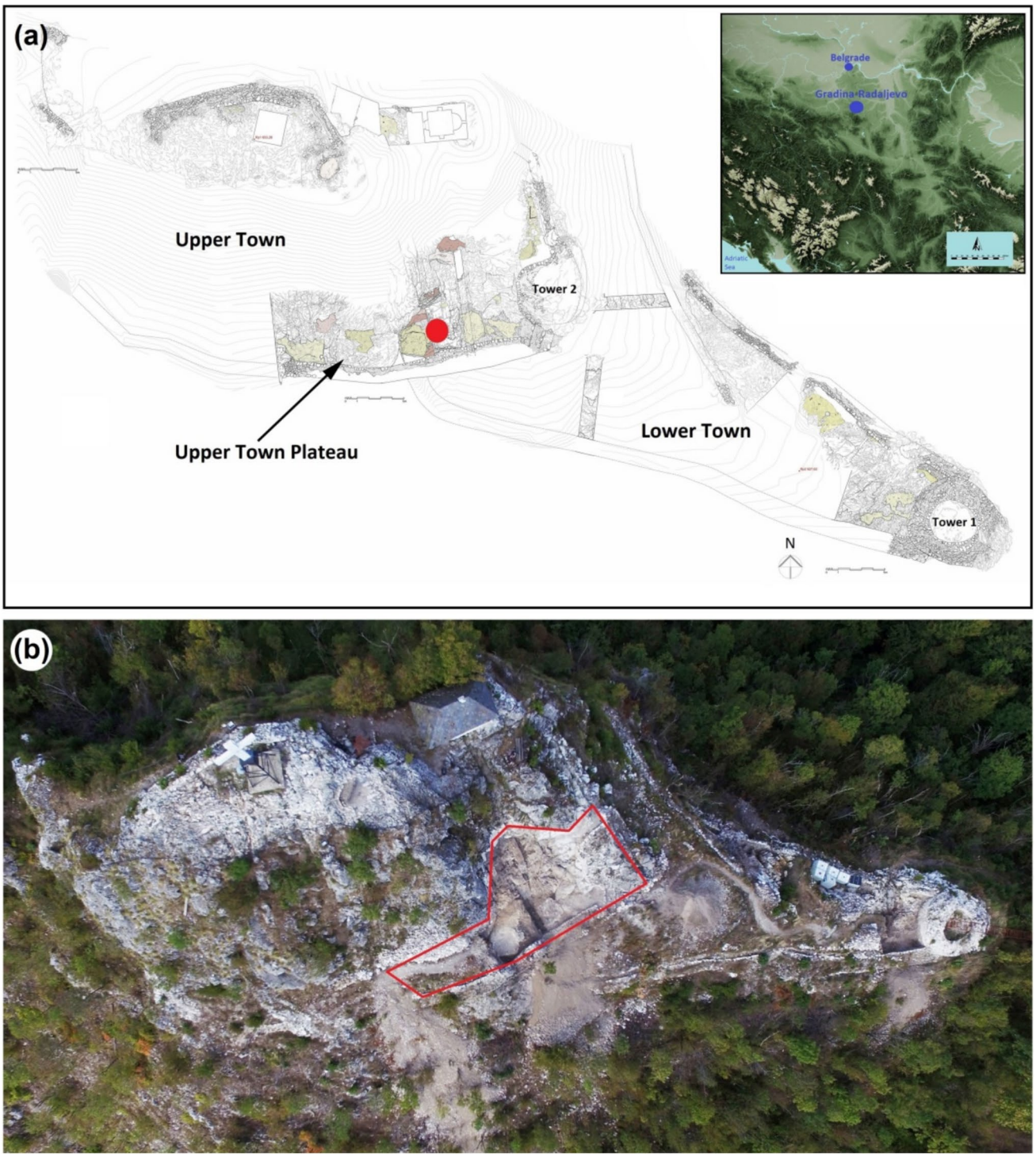

Fig. 1 (**a**) Location of the site on a map of the Central Balkans and site plan of the late medieval fortification at Gradina–Radaljevo – the red dot indicates the findspot and (**b**) orthophoto of the fortification – the area marked in red represents the excavated portion of the Upper Town Plateau

half of the fourteenth century based on two radiocarbon dates obtained from animal bones recovered within the same cultural layer as the paleofeces (lab no. DeA-35678; uncal. 584 ± 16 BP and lab no. DeA-35680; uncal. 571 ± 16) (Marković et al. 2023).

Methods

The multiproxy workflow implemented in this study comprises four main stages: non-invasive methods, invasive subsampling, metadata analysis, and presentation and

publication. Non-invasive methods include documentation through photography and macro-description, morphometric analysis, typological classification, stereomicroscopic surface analysis, and MicroCT scanning with 3D reconstruction. Invasive subsampling is conducted for paleoparasitological studies, and pollen analysis, followed by biomolecular analyses such as collagen peptide mass fingerprint (ZooMS) and ancient DNA (aDNA). Additional related techniques include scanning electron microscopy (SEM), thin section petrography, micro-Fourier transform infrared spectroscopy (μFTIR) and micro-X-ray fluorescence (micro-XRF). Finally, a comprehensive evaluation of the associated metadata is performed (Fig. 2).

Non-invasive methods

The first stage involved measuring the size and weight of the specimen, describing its shape, and classifying it according to Diedrich (2012), and Hunt and Lucas (2012). During this stage, a stereoscopic examination of the specimen surface was performed, and any visible macro-animal and/or plant remains were noted. In the second stage, micro-CT imaging and internal micromorphological analysis were conducted following the methodology of Romaniuk et al. (2020). MicroCT scanning was performed using a Nikon XTH 320 μCT scanner with a reflection target and settings of 160 kV and 58μA with a voxel size of 0.022138 mm and copper filter of 0.1 mm thickness. Post-processing of the scans was conducted using 3D Slicer software version 5.4.0, which is designed for professional medical examinations using the DICOM format. After the non-invasive recording the specimen was longitudinally halved using a circular diamond saw. Subsamples for various analyses were then taken with a sterile scalpel from the core of one half, avoiding the surface layer of the paleofeces.

Thin section petrography

The sample was prepared for petrographic analysis by first placing it in a 22 × 22 mm polyethelene container and embedding it using a slow setting epoxy resin (ProKlar). Upon curing, the cube was sliced approximately in half using a tile saw. The exposed cross-sections were photographed, and one piece was selected for analysis with micro-XRF. The analyses were conducted using a Bruker M4 Tornado tabletop instrument with a rhodium x-ray tube and dual detectors. Maps for single and multiple elements (Al, Ca, Cu, Fe, K, Mg, Mn, Na, P, S, Si, Ti, Zn) were produced from the entire cross-section under full tube power (30W) and vacuum (20 mbar) with a pixel spacing of 20 μm and a dwell time of 25 ms per pixel.

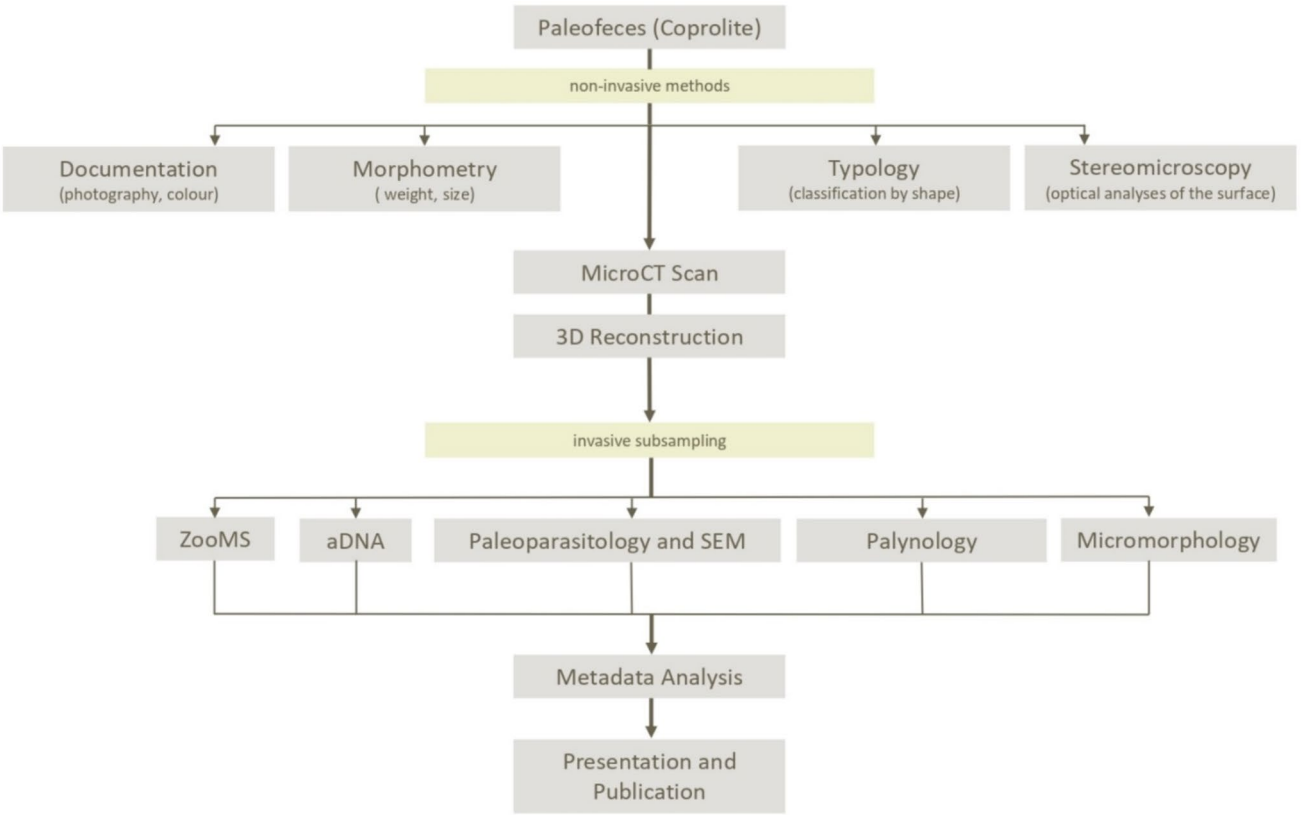

Fig. 2 Workflow scheme for multiproxy paleofeces analysis implemented in this study

Following micro-XRF mapping, the cross-section was mounted on a 51 × 76 mm glass slide and ground to a thickness of 30 µm. The resulting thin section was analyzed under plane- (PPL) and cross-polarized light (XPL) using a petrographic microscope. High resolution digital scans in SVS format were produced using a petrographic microscope equipped with a mechanical stage and the Microvisioneer AutoWSI software. A second micro-XRF scan was conducted on the thin section at this time. Finally, µFTIR analyses were conducted directly on the surface of the thin section in reflectance mode using an Agilent 610 FTIR microscope attached to an Agilent 660 bench. The resulting spectra were compared to an in-house reflectance database of common minerals and archaeological materials in thin section.

Petrographic analyses were integrated with the results of the micro-XRF and µFTIR analyses and compared to reference samples of modern, archaeological and paleontological feces from humans and other mammals (Goldberg 2000; Horwitz and Goldberg 1989; Mentzer 2018) that are housed in the Geoarchaeology collection at the University of Tübingen. When necessary, descriptive terminology followed guidelines that are specific to the archaeological micromorphology literature, such as Brönnimann et al. (2017) for paleofeces in general, Stoops (2021) for birefringence fabric, microstructure and voids, and Pümpin et al. (2017) for the identification of parasite eggs.

Paleoparasitology

A one gram sample was placed in a 15 ml test tube. Carbonates were dissolved using 10% HCl added dropwise until the end of the reaction. The solution was shaken gently to ensure full reaction. To remove the acid, distilled water was added, the tube centrifuged at 4,000 rpm for 5 min and the supernatant fluid removed, and this process repeated 5 times. After resuspension in distilled water, the sample was sieved through 300 µm, 160 µm, and 20 µm meshes. Sediment trapped on the 20 µm mesh was washed with distilled water and centrifuged for concentration (Ledger et al. 2019a; Rabinow et al. 2022). The final pellet was combined with glycerol, mounted on slides, and examined with light microscopy (200 × and 400x) to identify parasite eggs based on morphology (Garcia 2016). Microscope slides containing helminth eggs were thoroughly washed with distilled water in a 50 ml tube. The tube is then centrifuged at 4,000 rpm/5 min. After centrifugation, the supernatant was carefully pipetted off, and the pellet containing parasitic remains at the bottom of the tube was transferred to a 1.5 ml PCR tube. The sample was stored at −20 °C until the beginning of aDNA extraction. For scanning electron microscopy (SEM), ~ 30 µL of the prepared sediment sample was washed in ethanol, air-dried, and oven-dried at 42 °C, mounted on polycarbonate membranes with a 6 µm hole size, sputter-coated with gold, and examined using a Phenom XL Desktop Scanning Electron Microscope to capture images at magnifications up to × 3200 (Reinhard et al. 2019).

Palynology

The sample for pollen analysis was collected in volumes of up to 3 cm^3. This material was processed at the pollen laboratory of the Baden-Württemberg State Office for Cultural Heritage in Hemmenhofen. To estimate the concentration of the palynomorphs two *Lycopodium* tablets (i.e. exotic marker) with concentration 17,797 grains per unit were added to the sample together with 15 ml of 10% HCl to dissolve the carbonate rich matter of the paleofeces. The test tube with the solution were heated in water bath at 95 °C for 15 min and then centrifuged by 3600 pr. The supernatant was removed. As next in order to remove silicates ca. 8 ml of 48% HF (3) were added to each test tube and heated in water bath for 20 min. The treatment for pollen extraction does not follow the standard procedure (i.e. acetolysis) as this will destroy various relevant microfossils usually expected to be preserved in the paleofeces (Scott 1987). Subsequently the supernatant was removed and samples were rinsed with distilled water. The final residues were embedded in glycerin, stained with safranin and mounted on microscope slide. To reach a statistically representative palynomorph sum (~ 300 counted items) an additional 5 slides were prepared and analyzed under transmitted light microscope with magnification between 200—1000x.

ZooMS

Four samples (GACT1.G, GACT1.H, GACT1.I, and GACT1.J) of digested bone extracted from the matrix of the paleofeces during subsampling were analyzed following previously published protocols (Welker et al. 2016). In short, specimens were demineralised in 0.5 M HCl and rinsed in 50 mM ammonium bicarbonate. The demineralised bone chip was then gelatinised at 65 °C for one hour, and the resulting supernatant was treated with 0.4 µg trypsin (Thermo Scientific Pierce ™ Trypsin Protease). Enzymatic digestion took place at 37 °C for 18 h. The incubated samples were concentrated and desalted using C18 ZipTips (Thermo Scientific Pierce™ C18 Tips) and eluted in a final solution of 50 µl of 50% acetonitrile and 0.1% TFA. 0.5 µl of the resulting solution was mixed with 0.5 µl of α cyano-4-hydroxycinnamic acid solution (10 mg/mL in 50% acetonitrile and 0.1% trifluoroacetic acid), spotted in triplicate on an MTP384 groundsteel plate, and allowed to crystallise.

Samples were analysed in the Archaeo and Palaeoproteomics Laboratory at the University of Tübingen using a Bruker AutoFlex LRF Speed. The resulting spectra were peak picked with a signal to noise ratio of 3.5 after baseline correction, smoothing, and deisotoping following our in-house parameters (Brown 2021) and analysed with flexAnalysis 3.4 (Bruker Daltonics) and mMass software (Strohalm et al. 2008). The spectra were compared against a reference library of known peptide markers (Buckley et al. 2009, 2010; Codlin et al. 2022; Eda et al. 2020; Welker et al. 2016) and reported following standard ZooMS nomenclature (Brown et al. 2021).

Ancient DNA

aDNA analyses were performed to identify the paleofeces source, detect dietary components and investigate the potential presence of parasitic taxa, providing insights into the animal's health. We extracted aDNA from two different components of the same specimen: a subset of the paleofeces (RADA001.A), and isolated parasite eggs previously identified microscopically (RADA001.B). A subset of ~ 200 mg from the paleofeces was extracted using a modified Dabney protocol (Dabney et al. 2013), which was found to outperform other extraction methods on paleofeces (Hagan et al. 2020). A single-stranded, double-indexed, non-UDG treated library was then prepared following an established protocol for degraded aDNA (Gansauge et al. 2020). Negative and positive controls, the latter consisting of cave bear (*Ursus spelaeus)* bone powder, were included.. After DNA amplification and dilution, the library underwent shotgun sequencing for around 30 million single end reads on an Illumina sequencing platform.

Sequencing data were pre-processed and mapped competitively against nuclear and organelle reference databases using nf-core/eager (Fellows Yates et al. 2021) and the HOLI pipeline (Pedersen et al. 2016), with damage rates estimated via metaDMG (Michelsen et al. 2022; for full parameters, see Supplementary File 1). Taxonomic identifications required ≥ 10 mapped reads, ≥ 5% terminal deamination, and a statistically significant deamination pattern relative to the reference. Putative hits below 100 reads were further validated by BLASTn against the 'nt' database ('nt' database, August 2025).

Results

Results of non-invasive methods

These non-invasive techniques provided critical structural and compositional insights prior to any physical sampling, ensuring the preservation of the specimen's integrity during the initial analysis. The analyzed paleofeces exhibits a flat-conical shape and presents a surface coloration in various shades of gray. Macroscopically, several digested bone fragments are visibly embedded in the external matrix. Stereomicroscopic examination revealed additional, smaller bone particles with advanced stages of digestion. Morphologically, the specimen corresponds to Type A, characterized by a compact structure and flattened base, with the following dimension – length: 49.7 mm, width: 41.3 mm, height: 28.5. mm, and weight of 19.8 g (Fig. 3a–d).

Three-dimensional microCT analysis provided detailed insights into the internal composition. The interior of the paleofeces contains both trabecular and compact bone fragments, suggesting a carnivorous digestive process. Additionally, the microCT revealed large empty voids, consistent with gas escape or soft tissue decomposition during fossilization, as well as highly calcified regions, suggesting post-depositional mineral alteration or prolonged gut retention (Fig. 3e–g) (Tripp et al. 2022).

Thin section petrography and associated microanalyses

In thin section, the paleofeces exhibits a porous structure with numerous aligned moldic voids. The outer surface is not present and cannot be observed. The inner matrix is pale yellow under PPL with a crystallitic birefringence fabric under XPL (Fig. 4a–c). The main elemental composition of the matrix is P (Fig. 4d–e) and Ca, with µFTIR spectra indicating the mineral hydroxylapatite. A number of inclusions were also observed (Fig. 4f–g). The largest fragments consisted of a piece of cancellous bone, nearly 5 mm in diameter. An additional 39 fine and medium sand-sized fragments of bone were also observed with lengths ranging from 150 µm to one mm. Smaller pieces were also present but were not counted. Most bones are pale yellow to transparent in PPL with low order grey interference colors in XPL. The edges of some fragments and a few smaller pieces are strongly yellow in PPL and isotropic in XPL. µFTIR spectra of the 15 largest bones indicate peaks typical of carbonate hydroxylapatite, with dominant peaks at 1030 cm—1, 874 cm—1, and a doublet at 605 and 565 cm—1. Peaks that appear due to high temperature heating, in particular those at 1088 cm—1 and 630 cm—1 were not present. Charcoal fragments were also observed, the largest of which is 0.7 mm long. Mineral inclusions consist of fragments of quartz, feldspar, calcite and rocks, as well as one aggregate of soil, all ranging in size from 20—180 µm in diameter.

Moldic voids preserve the morphology of other organic components that have since decomposed or were otherwise removed during sample preparation. These voids are

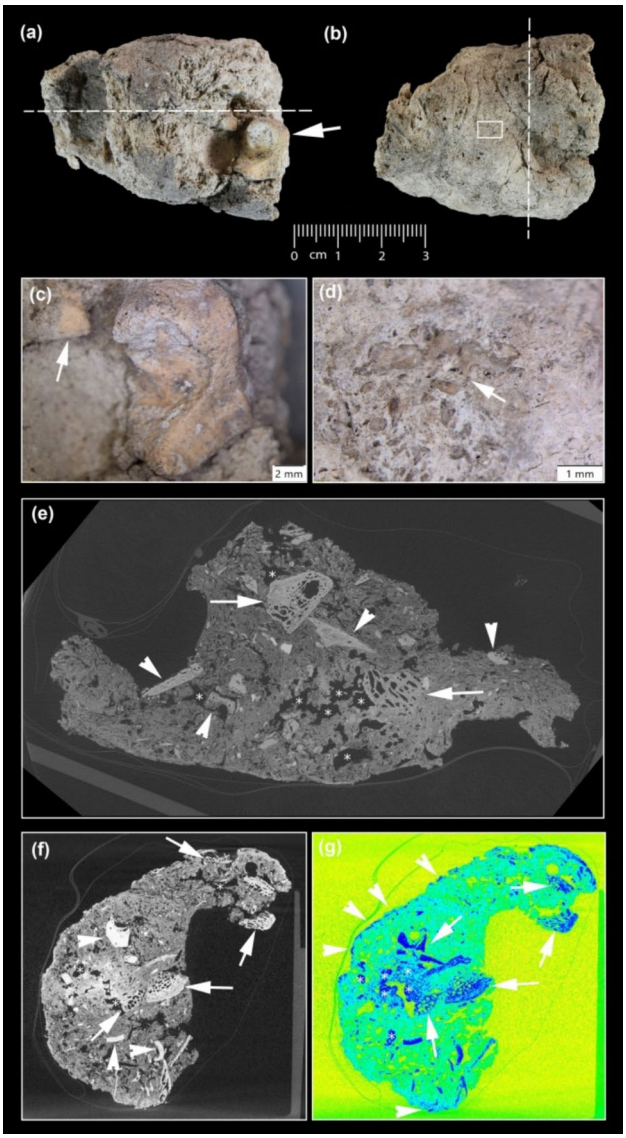

Fig. 3 Dog paleofeces from the late medieval fortification at Gradina–Radaljevo: (**a**) and (**b**) show opposite sides of the same specimen; (**a**) arrow indicate areas shown at higher magnification in (**c**) and the dashed line indicates the location of the longitudinal microCT section shown in (**e**); (**b**) the box highlights the area shown at higher magnification in (**d**) and the dashed line indicates the location of the transverse microCT section shown in (**f**); (**c**) the box reveals a higher magnification of a larger fragment, and the arrow indicates a smaller fragment of digested bone visible on the surface; (**d**) higher magnification of a group of bone fragments visible on the surface of the specimen indicate by arrow; (**e**) the longitudinal microCT section reveals some of trabecular (arrows) and compact digested bones (arrowheads), as well as cavernous space (asterisks); (**f**) the transversal microCT section reveals some of trabecular (arrows) and compact digested bones (arrowheads), as well as cavernous space (asterisks); (**g**) false color map of the same section in (**f**) reveals fragments of digested bones (arrows), outer line of paleofeces with higher mineral density (arrowheads) and core part with higher mineral density (asterisks)

typically elongate and slightly concave, with smooth sides and either sharp or tapering ends. Widths are typically 50—70 µm with a circular cross-section. Some exhibit spiral morphologies. A majority of the voids are consistent in morphology with grain husks (Nicosia and Canti 2017), which also exhibit smooth sides with both sharp and tapering ends when cut along a longitudinal plane. Moreover, when cut along a transverse plane, husks exhibit a characteristic "spiral-like" morphology (Nicosia and Canti 2017: Fig. 14.2). Some elongate moldic voids contain phytoliths in their centers, and some more equant voids also contain remnants of humified plant material. These observations suggest that many of the voids in the sample derive from decayed plants (vegetal voids). The shapes of some thinner voids are also consistent with decomposed hair and fur ("negatives" or "hair pseudomorphs") following Brönnimann et al. (2017). Omnivores and carnivores can ingest hair and fur along with their prey, or during grooming activities.

Additional post-depositional processes include localized reddish staining of the matrix around charcoal fragments, a process that is also reported in a dog paleofeces analyzed (Brönnimann et al. 2017: Fig. 7.10). A darker region of the sample under PPL was observed to be enriched in Mn and Zn in the elemental distribution maps, which is suggestive of the formation of post-depositional manganese oxides.

Paleoparasitological results

Light microscopy of one gram of mineralized paleofeces sample revealed a total of 26 intestinal parasite eggs. These eggs were assigned to three distinct taxa based on their morphometrical characteristics.

Nine of the eggs were identified as belonging to the genus *Ascaris* sp., a common nematode (roundworm). These eggs are subspherical to oval in shape, measuring approximately 61.4 µm (standard deviation ± 3.5 µm, n = 9) in length and 46.2 µm (SD ± 2.8 µm, n = 9) in width (Supplementary File 2 – Table S1). Six of them possess a thick shell, with the outermost layer appearing mammillated (Fig. 5a). Three specimens showed loss of the outer coat, revealing a smoother underlying layer (Fig. 5b). These morphological traits are consistent with those described for the eggs of *Ascaris* sp. affecting humans (*Ascaris lumbricoides*) and pigs (*Ascaris suis*) in both modern and archaeological contexts (Garcia 2016; Ledger et al. 2025).

Six eggs displayed characteristics typical of the whipworm (*Trichuris* sp.). These eggs are distinctive in morphology, being lemon- or barrel-shaped. The eggs have a smooth, yellow–brown shell and a thick wall, which aids in preservation

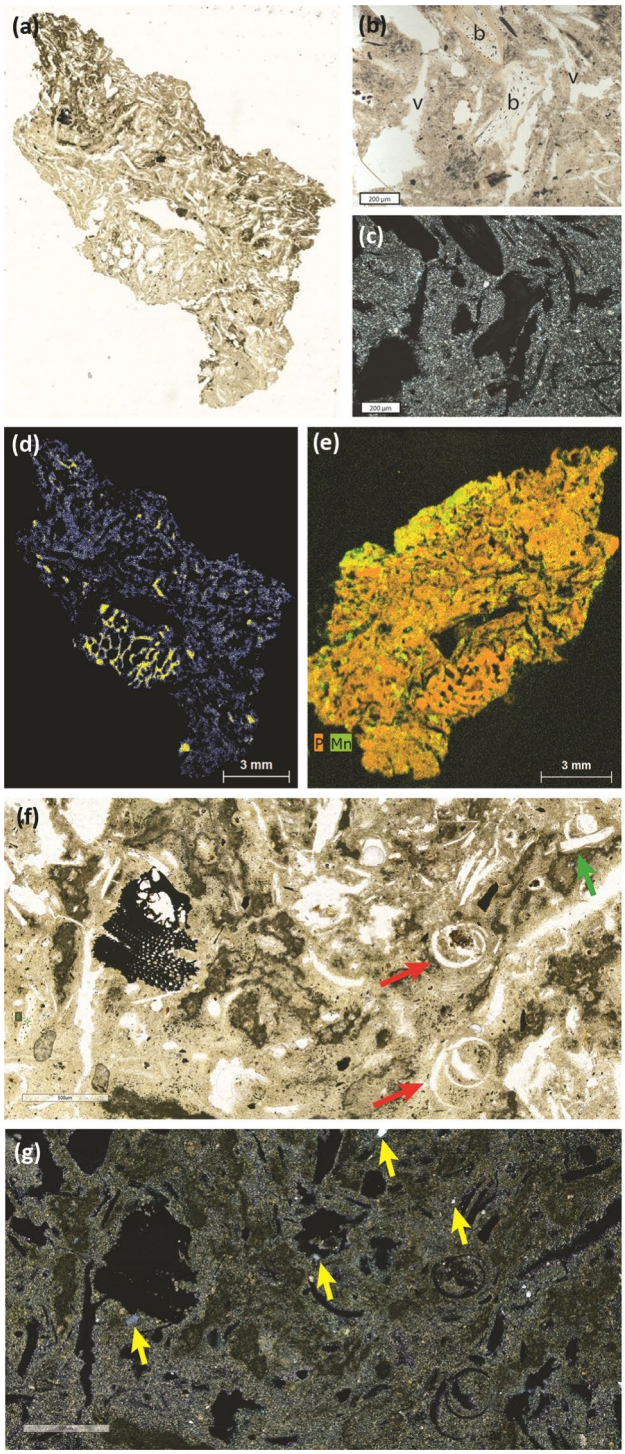

Fig. 4 The paleofeces in thin section: (**a**) photomosaic image of the sample under PPL with the highly porous fabric visible; (**b**) higher magnification view of the yellow matrix, two bone fragments—b and moldic voids – v; PPL; (**c**) same view as (**b**) in XPL, showing the crystallitic birefringence fabric; (**d**) micro-XRF analyses—elemental scan of the sliced face prior to thin section production showing the distribution of P and Mn. P is present throughout both the matrix and in bone inclusions. Mn is concentrated along one edge of the fragment; (**e**) a false color image generated from a map of the sample in thin section, showing areas where P is present ranging in color from blue (lowest abundance) to yellow (highest abundance). Yellow areas correlate in thin section with bone fragments that are approximately larger than 150 µm (fine sand). A large fragment of cancellous bone is visible; (**f**) Inclusions and moldic voids – large fragment of charcoal is visible in the left of the image. White areas are voids, with red arrows indicating two voids with spiral morphology and tapering ends. The upper of the two spiral voids surrounds a fragment of humified plant material. The green arrow indicates an elongate void with blunt ends. These voids have morphologies consistent with cereal husks; PPL; (**g**) same view as (**f**) in XPL – the yellow arrows indicate quartz grains

over archaeological timescales. Only one has preserved mucus plugs on both poles (Fig. 5c). The other five have no preserved mucus plugs (Fig. 5d). Measurements ranged from 48.1 µm (standard deviation ± 5.2 µm, n = 6) in length and 23.2 µm (standard deviation ± 0.7 µm, n = 6) in width (Supplementary File 2 – Table S1). The dimensions and features observed are consistent with those of *Trichuris* sp. that infect humans (*T. trichiura*) and pigs (*T. suis*) (Rabinow et al. 2022).

The remaining eleven eggs were consistent in morphology with those of small flukes, likely trematodes of the family Dicrocoeliidae, more precisely *Dicrocoelium* sp. They were ovoid in shape, with one lateral side slightly flattened, smooth and thick-shelled, and light to dark brown coloration. Six of the eggs retained a well-preserved operculum, while the remaining five lacked this feature, possibly due to post-depositional degradation (Fig. 5e–f). The eggs measured approximately 35.6 µm (standard deviation ± 3.3 µm, n = 11) in length and 26 µm (SD ± 1.1 µm, n = 11) in width (Supplementary File 2 – Table S1). Scanning Electron Microscope (SEM) examination confirmed the morphometric data observed under the light microscope by revealing two of the eggs (Fig. 5g–h).

Palynological results

The pollen analysis revealed a modest concentration of pollen and spores (ca. 1000 per 1 cm^3) and nearly the same abundance of plant tissue fragments (Fig. 6a–b; Supplementary File 2 – Table 2). In total it was possible to identify 25 different pollen and spore taxa, and 4 non-pollen-palynomorphs (NPP). The assemblage is dominated by representatives of the non-arboreal vegetation, like sedges (Cyperaceae), grasses (Poaceae) and fern spores and over quarter of the pollen finds are unidentifiable due to bad preservation and corrosion. Only few representatives of the potential natural vegetation near the site, deciduous oak woodland, were also registered, dominated by the pollen of the light-demanding hazel (*Corylus*). Of interest are the two large pollen grains of Cerealia-type – the pollen type including cultivated cereals. Nearly half of all microfossils found belong to plant tissues, mostly such from epidermal tissues and conifer wood, obviously ingested by the carnivore, which produced the paleofeces (Fig. 6c–d). The NPPs belong mostly to aquatic or humid

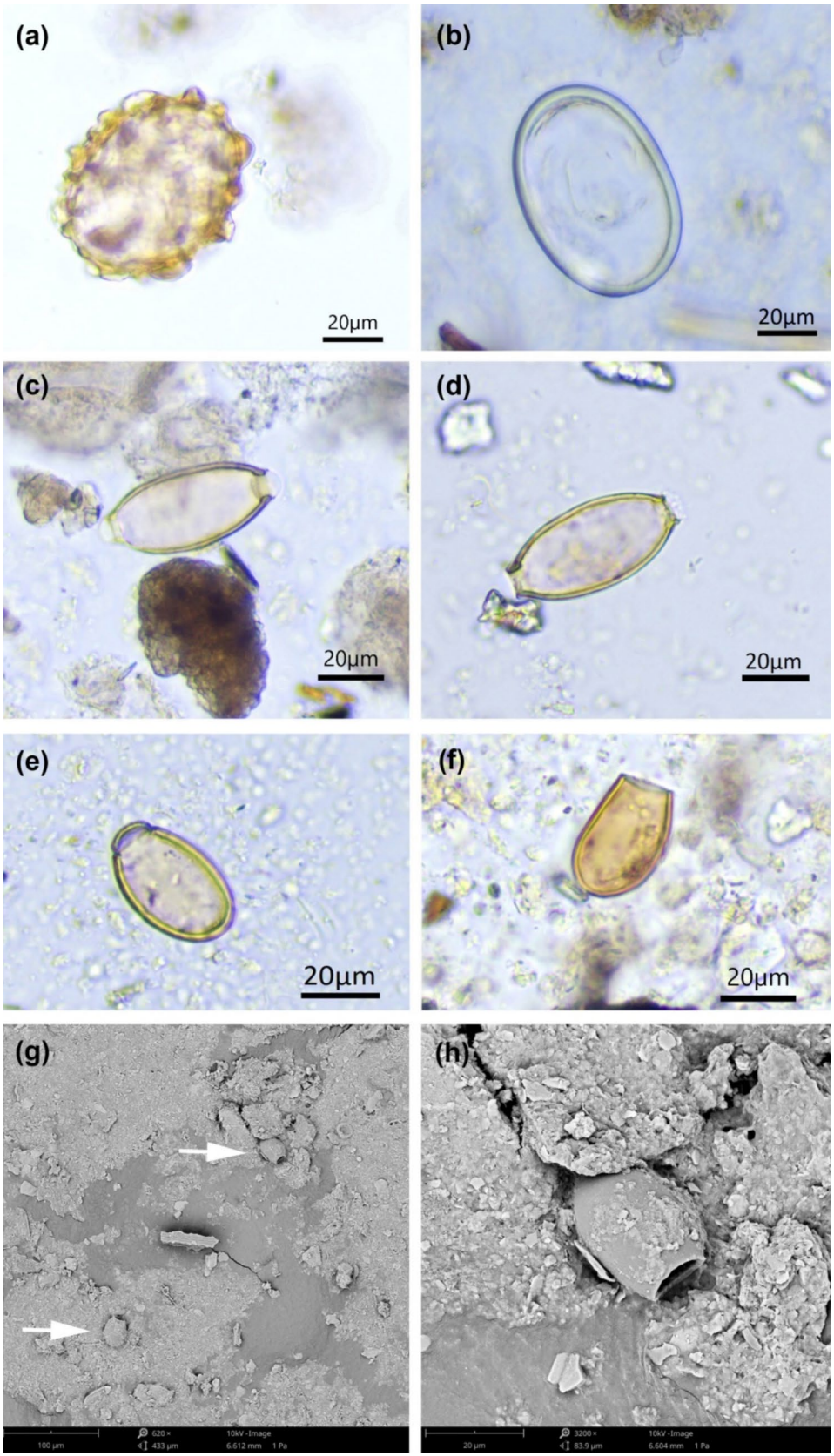

Fig. 5 Parasite eggs from three different taxa identified by microscopy in dog paleofeces from the Gradina–Radaljevo: (**a**) fertilized roundworm (*Ascaris* sp.) egg with mamillated coat and (**b**) fertilized decorticated egg of the roundworm (*Ascaris* sp.); (**c**) whipworm (*Trichuris* sp.) egg with preserved mucus plugs at both poles and (**d**) egg of whipworm without preserved mucus plugs; (**e**) *Dicrocoelium* sp. egg (probable Lancet liver fluke) with preserved operculum and (**f**) *Dicrocoelium* sp. egg without preserved operculum; (**g**) and (**h**) eggs of *Dicrocoelium* sp. under scanning electron microscopy (SEM)

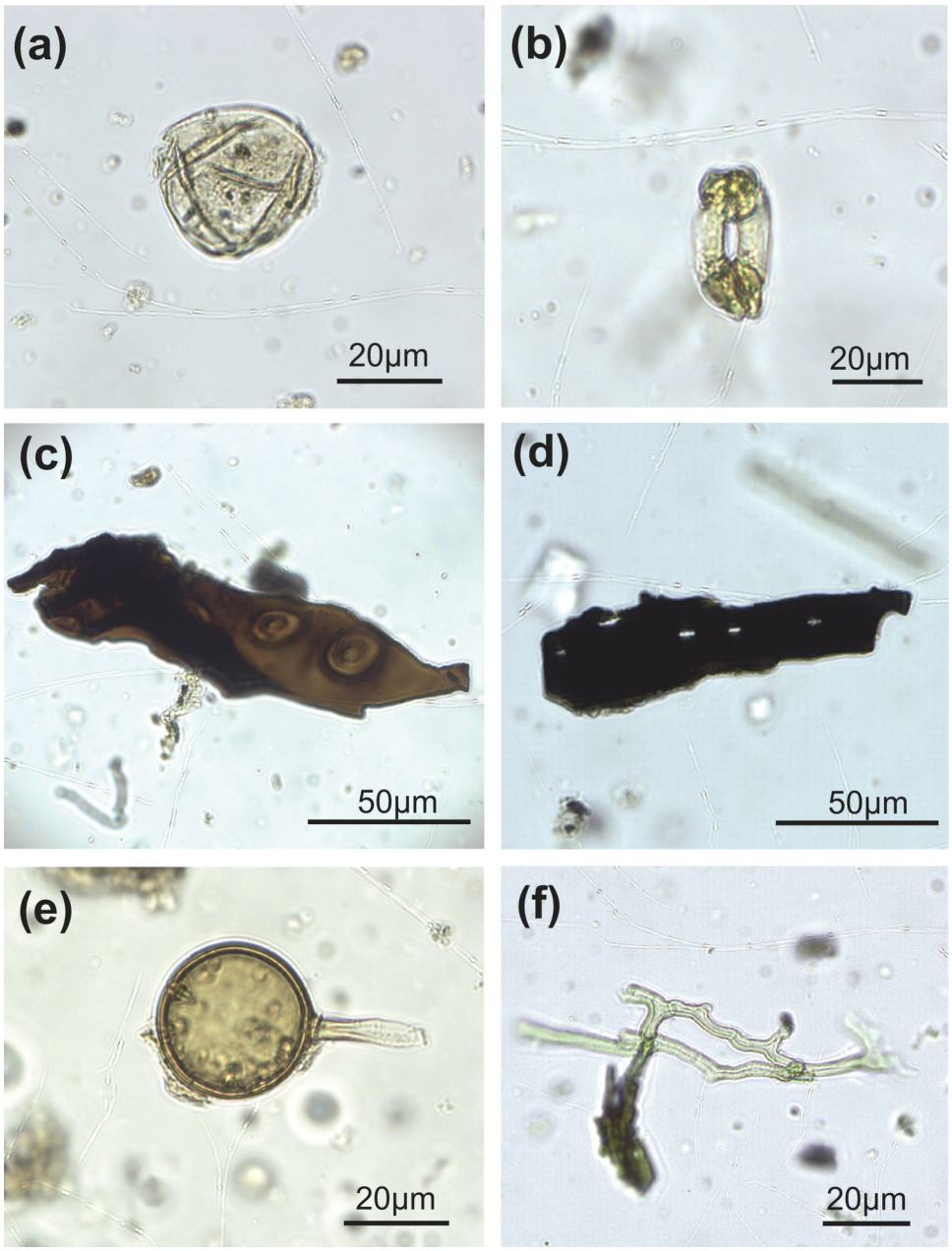

Fig. 6 Key microfossils from the palynologcal samples: (**a**) *Juniperus* pollen; (**b**) conifer stomata, cf. Juniperus; (**c**) conifer wood fragment; (**d**) charred particle probably of plant origin; (**e**) HdV Type 207 (*Glomus* sp., chlamydospore); (**f**) fungal hyphae

environments (testate amoebe and HdV 128 and 225) (Pals et al. 1980). An exception is the HdV 207-type Glomus sp., an endomycorrhizal fungus (Fig. 6e–f) (Geel et al. 1989).

ZooMS

Sufficient collagen was extracted from all four of the bone fragments obtained from within the paleofeces, allowing for their taxonomic identification. Two (GACT1.G and GACT1.J) contained peptides consistent with the identification of Suidae, using a combination of seven peptides to confirm this identification (Buckley et al. 2009; Welker et al. 2016). A further two samples (GACT1.H and GACT.I) were consistent with Aves and most specifically match to *Gallus gallus* (Eda et al. 2020; Codlin et al. 2022). ZooMS reference libraries for birds are underdeveloped in comparison with mammals and differentiating between Aves taxa typically requires a greater number of peptide markers for a confident identification. In this instance we used a combination of ten peptide markers for the assignment of *G. gallus* including peptide COL1α2 889–906 which at present has a unique amino acid sequence and marker to the group (1604.8 m/*z* and 1620.8 m/*z* with a hydroxyproline). With the growth of ZooMS reference libraries, it may be determined that this is not a unique *G. gallus* marker and the identification will need to be revisited (Supplementary

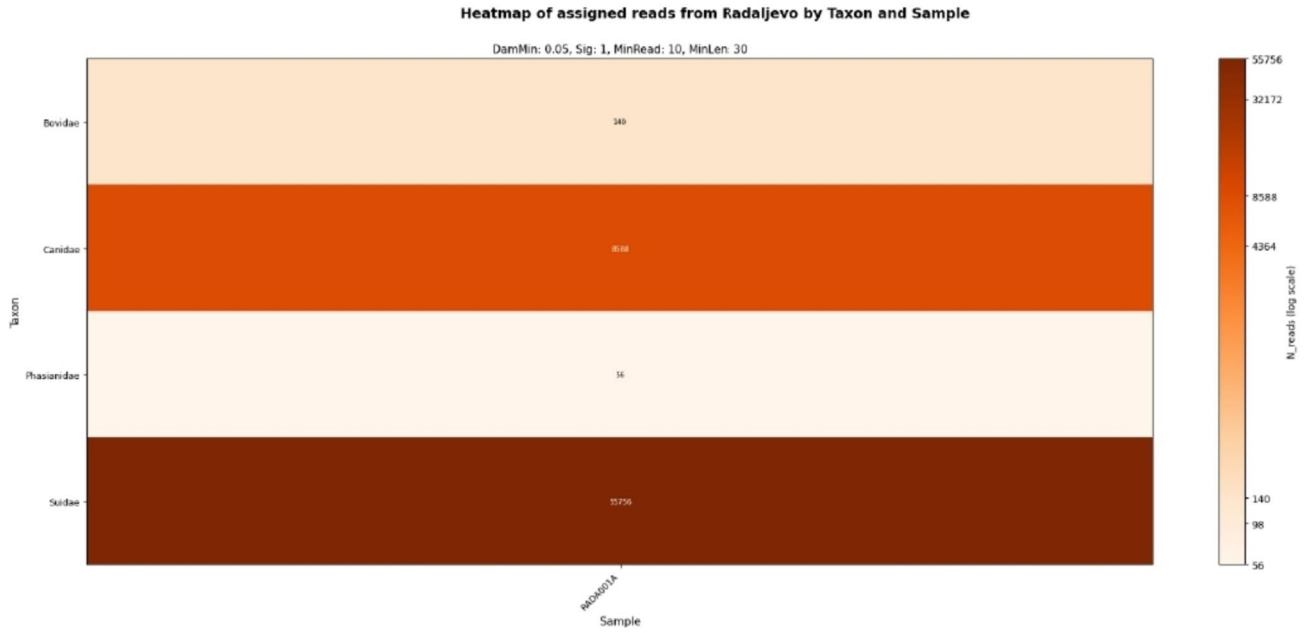

Fig. 7 Heatmap illustrating the distribution of assigned reads per taxon in the paleofeces sample RADA001.A. Log-transformed read counts are shown by the color gradient, with numerical values indicating the actual assigned reads following metagenomic analyses

File 2 – Table 3; Supplementary File 2). This interpretation, however, aligns well with the zooarchaeological evidence from the site, where domestic pig and chicken bones were identified (Bulatović and Marković 2013).

aDNA

In the library obtained from the DNA extract of the paleofeces fragment (RADA001.A) we identified five taxa at the family level. Among them Suidae, Canidae, Bovidae and Phasanidae with a minimum of 5% damage on the terminal ends and a minimum significance of 1 (Fig. 7). One taxon, Lipotidae, had to be excluded after the subsequent authentication steps, as none of the reads were assigned to Lipotidae with BLASTn. The taxonomic resolution varies among these taxa. This is due to differences in their representation within the reference databases, as well as variation in the abundance of their genetic material within the sample.

For Bovidae, as well as Phasianidae, only an identification to family level was possible. For Canidae, two species were identified, *Vulpes vulpes* and *Canis lupus*. For *C. lupus* the best sub-species candidate was assessed to be *C. lupus familiaris* (the domesticated dog). The Suidae represented in this sample was identified to species level as *Sus scrofa*, with the only identified candidate on subspecies level being *S. scrofa domesticus* (the domestic pig). For the full assessment of the taxonomic resolution see Supplementary File 1.

Ancient DNA extraction followed by library preparation was also attempted on parasite eggs isolated from the same paleofeces (RADA001.B). The presence of aDNA signatures from nematode, platyhelminth, or other parasitic taxa were not confirmed (for further identification steps on the parasitic taxa; see SI 1). Notably, the identified animal taxa match those obtained from the paleofeces sub-sample RADA001.A. Negative controls processed alongside the samples yielded no detectable taxonomic signal.

Discussion

The paleofeces analyzed in this study represent a rare and exceptionally well-preserved example of dog excrement from a medieval settlement. Its identification relied on a stepwise, multidisciplinary workflow, in which the physical appearance of the specimen constituted the initial and essential line of evidence. Macroscopic morphology provided the first indication of a canid origin, which was subsequently supported by micro-CT imaging and internal micromorphological assessment. Targeted subsampling for biomolecular and parasitological analyses further corroborated this interpretation. Taken together, these complementary lines of evidence allow the specimen to be confidently identified as dog paleofeces, providing valuable insights into past animal behavior, parasite ecology, and human–animal interactions. The results integrate palynological, petrographic, and paleoparasitological evidence to reconstruct aspects of diet, environment, and parasite transmission pathways (Supplementary File 1; Fig. 5).

Comparative analysis distinguishes carnivore, herbivore, and human paleofeces based on composition and morphology. Carnivore paleofeces typically contain a high proportion of digested bone, are compact, and often show intense mineralization. Herbivore paleofeces are fibrous, loosely compacted, and lack bone inclusions, reflecting a plant-based diet. Human paleofeces usually present mixed contents, including plant fibers, seeds, and occasional bone fragments, and are often elongated or cylindrical (Tolar et al. 2021; Tolar and Galik 2019). Based on the presence of extensively digested bone, the flat-conical morphology, and the internal microstructural features identified via micro-CT, this specimen is attributed to a carnivorous origin. The ancient DNA results revealed signatures of three animals—*Sus scrofa*, *Vulpes vulpes*, and *Canis lupus*—all of which are omnivorous and occasionally engage in coprophagy. This complicates host assignment if relying solely on genomic evidence. Moreover, without targeted enrichment, taxonomic resolution below the family level remains tentative and must be corroborated through multiple lines of evidence. Several microbial taxa detected in the specimens resemble an expected mixture of environmental and gut microbial DNA (Supplementary File 1; Fig. 5).

ZooMS and aDNA analyses also identified pig and bird biomolecular traces, likely derived from kitchen waste, and a bovid signature probably linked to dietary intake (Liu et al. 2021). Importantly, although both ancient dog and fox DNA signatures were present, the integration of multiple proxies—morphology, micromorphology, ZooMS, and ancient DNA—supports attribution to a dog host. The fox is considered less likely because its genetic signal is weaker and inconsistent with the morphological and micromorphological characteristics of the specimen. In this way, the host assignment relies on the convergence of multiple independent lines of evidence, demonstrating the value of a multidisciplinary approach for confident interpretation of complex archaeological samples.

Microscopic analysis revealed parasite eggs belonging to three taxa—*Ascaris* sp., *Trichuris* sp., and *Dicrocoelium* sp.—with a total of 26 eggs identified. Although this tri-parasitic assemblage is noteworthy, several lines of evidence indicate that these remains represent false parasitism rather than true infection of the dog. First, the overall egg counts are very low, with only 26 eggs recovered. In genuine intestinal infections of dogs, parasite eggs are typically present in much larger numbers per gram of feces. Such low counts are therefore more consistent with accidental ingestion and passive passage through the digestive tract. Second, the identified nematode eggs do not correspond to typical canine parasites. The *Ascaris* and *Trichuris* eggs correspond morphometrically to species infecting humans and pigs (*Ascaris lumbricoides/suum* and *Trichuris trichiura/suis*) (Leles et al. 2012; Liu et al. 2012), rather than to species commonly infecting dogs, such as *Trichuris vulpis*. Both *Ascaris* and *Trichuris* are frequently encountered in archaeological contexts and reflect the close ecological relationships among humans, livestock, and dogs in medieval settlements (Bouchet et al. 2003; Dufour and Le Bailly 2025; Mitchell 2015). Their presence in dog feces is therefore plausibly explained by the ingestion of human or animal feces (coprophagy) or contaminated food waste (Shalaby et al. 2010). Although cross-infection between humans, pigs, and dogs has been documented, the combination of host specificity and low egg abundance strongly suggests that the dog functioned as an accidental carrier rather than a true host.

The presence of *Dicrocoelium* sp. eggs provides additional support for this interpretation. Eggs of *Dicrocoelium dendriticum*, the lancet liver fluke, are small, ovoid, operculated structures typically measuring 35–45 µm in length and 20–30 µm in width. They possess a smooth, brownish shell and a distinct operculum at one pole, features that facilitate their identification. These eggs are usually embryonated when passed in feces, although their internal structures may not always be visible under archaeological taphonomic conditions (Mehlhorn 2016; Roberts and Janovy 2008; Eskew et al. 2019).

Importantly, *D. dendriticum* primarily infects herbivorous mammals such as sheep, cattle, and goats, with terrestrial snails and ants serving as intermediate hosts (De Cupere et al. 2022; Graff et al. 2020; Ledger and Mitchell 2022; Rabinow et al. 2024; Slepchenko et al. 2025b). Because canids are not suitable definitive hosts for this parasite, its occurrence in dog feces is most plausibly explained by the consumption of infected herbivore viscera or offal, likely obtained through scavenging of butchery waste in a medieval settlement context. In this case, the eggs would represent material that simply passed through the digestive tract without establishing infection. Taken together—the low egg counts, the absence of typical canine parasites, and the host specificity of the identified taxa—these observations strongly support the interpretation that the parasite assemblage reflects false parasitism resulting from coprophagy or scavenging behavior, rather than genuine parasitic infection of the dog.

Palynological and petrographic analyses provide a complementary reconstruction of the dog's diet and surroundings. The low concentration of palynomorphs aligns with expectations for carnivores, ingesting pollen mainly via environmental exposure rather than direct plant consumption. Pollen of *Alnus*, *Salix*, *Persicaria maculosa*, *Cyperaceae*, and *Polypodium*, alongside testate amoebae (*Centropyxis ecornis*) and freshwater indicators, suggest ingestion of microfossils through drinking water. The broader spectrum,

dominated by grassland, meadow, and ruderal taxa, reflects an anthropogenically modified landscape. Cereal pollen and other human-associated indicators imply incidental consumption of food waste and confinement near the settlement during paleofeces formation. Scarce oak pollen and low overall concentrations point to deposition in late autumn or winter. Abundant plant tissues, charcoal, *Juniperus* pollen, and conifer fragments suggest ingestion of kitchen waste, possible ethnoveterinary treatment of canine ailments (Stucki et al. 2019). Mycorrhizal fungal spores (*Glomus* sp.) indicate intake of soil components. Collectively, these proxies reveal an omnivorous, opportunistic diet typical of free-ranging or semi-domesticated dogs closely linked to human settlements and waste areas.

Micro-CT and thin section petrography together enabled visualization of organic and inorganic inclusions, fabric, and matrix composition. Micro-CT provided non-destructive imaging of the overall structure but lacked resolution for small inclusions, such as moldic voids after decomposed plants. In contrast, thin section petrography with in situ microanalyses (micro-XRF, µFTIR) allowed detailed observation of silt-sized mineral grains, bone fragments, and hair-shaped voids, albeit destructively and in a single cross-section. Despite limitations, petrography revealed bone, charcoal, humified plant tissues, and mineral inclusions. µFTIR showed that bones were not highly burned, while charcoal and vegetal voids indicate ingestion of both fresh and heated materials. These data suggest scavenging from hearths, ovens, or kitchen middens, possibly the same context where the paleofeces was recovered. Mineral grains likely entered through soil ingestion during feeding (Brönnimann et al. 2017). The sample's structure and inclusions confirm fecal material from an omnivore. Unlike some comparative examples, vesicles and fecal spherulites were absent (Canti 1999). Two possible parasite eggs—ellipsoidal (Pichler et al. 2014; Pümpin et al. 2017), >20 µm with brown margins—were noted, though identification was limited by section orientation and magnification.

Conclusions

The integrated parasitological, palynological, petrographic, and microanalytical data indicate that the dog producing the paleofeces was an omnivorous scavenger living within or near the medieval settlement, feeding on human refuse, soil, and possibly fecal material. Its diet contained both animal and plant remains, burned food scraps, fragmented bone, cereal husks, and other domestic waste, consistent with opportunistic scavenging and coprophagy. The presence of parasite eggs is best explained by indirect ingestion rather than true infection: *Ascaris* and *Trichuris* reflect human parasitism, while *Dicrocoelium* derives from local herbivores, showing how dogs served as passive carriers or mechanical vectors rather than definitive hosts. Low egg concentrations and the absence of canine-specific helminths such as *Toxocara canis* and *Ancylostoma caninum* further support false parasitism rather than active infection (Dias et al. 2013; Nijsse et al. 2015). Environmental microfossils, including *Glomus* spores, wetland pollen, and abundant soil particles, demonstrate indirect uptake through contaminated food and sediment, reinforcing the need for caution in interpreting paleoparasitological evidence and distinguishing true infection from incidental passage. The multidisciplinary approach, combining microscopy, palynology, petrography, and aDNA analysis, enabled a nuanced interpretation of the specimen. Microscopy proved essential in detecting and identifying all three parasite taxa, illustrating the continued relevance of morphological techniques in mineralized, degraded, or low-DNA preservation contexts.

Ultimately, this dog paleofeces provides an exceptional window into medieval parasite ecology, highlighting the research potential of paleofeces in revealing complex relationships between humans, domestic animals, and surrounding landscapes. The parasite assemblage, diet traces, and microfossil content collectively portray a scavenging dog actively engaged in waste consumption and soil components ingestion, thereby documenting both animal behavior and the broader health and sanitation landscape of the community. So far, the presence of carnivores (dogs) at the site has been inferred only indirectly, based on gnawing marks observed on animal remains (Bulatović and Marković 2013). The paleofeces thus serves as a proxy archive of daily life, disease circulation, and human–animal entanglements in the medieval settlement. This multiproxy workflow demonstrates a high-resolution, ethically sensitive framework for extracting maximal biological, ecological, and cultural information from rare paleofeces specimens, offering a model for future studies seeking to reconstruct past human–animal relationships and sanitary landscapes.

Supplementary Information The online version contains supplementary material available at https://doi.org/10.1007/s12520-026-02499-1.

Acknowledgements We would like to thank Panagiotis Kritikakis for producing the thin sections, Tatiana Miranda for preparing the SEM samples, and Gerlinde Bigga for the graphic design of Figure 2.

Author contributions N.M. conceived and designed the study, performed data collection and analysis, and made the major contribution to writing and interpretation of the manuscript. F.S., E.M., S.B., S.M., C.M., and D.B. performed analysis and contributed to writing and interpretation. M.S., V.F.R., and E.R. performed analysis. M.R. contributed to writing and interpretation. P.M. and C.P. supervised the study and contributed to writing and interpretation. All authors read and approved the final manuscript.

Funding This research is a result of the project *Parasitism and Pleistocene Human Palaeoenvironment in the Western Balkans: Establishing a Multidisciplinary Protocol*, funded by the Leibniz ScienceCampus 'Geogenomic Archaeology Campus Tübingen (GACT)' (project number W73/2022) supported by the Leibniz Association, the Ministry of Science, Research, and the Arts of Baden-Württemberg and the University of Tübingen.

Data availability The sequenced raw reads from the analysed sub-samples of the coprolite are available at the European Nucleotide Archive under the accession number PRJEB112570. All other primary data produced as part of this study is available within the Supplementary Information.

Code availability Not applicable.

Declarations

Ethics approval Not applicable.

Consent for publication Not applicable.

Competing interests The authors declare no competing interests.

References

Slepchenko S, Ostapenko S, Khrustalev A, Kashevskaya A, Tretyakov N, Bull I (2025b) Archaeoparasitological and biomolecular analysis of the wells from the Black Sea city of Phanagoria during the Khazar Period (8th–9th centuries A.D.). *Parasitology*: p 1–35. https://doi.org/10.1017/S0031182025100929

Barbera A, Reinhard K (2024) Archaeoparasitology. In: Nikita E, Rehren T (eds) Encyclopedia of Archaeology, 2nd edn, Vol. 2B. Academic Press, p 827–838. https://doi.org/10.1016/B978-0-323-90799-6.00014-8

Blong J, Shillito L-M (2021) Coprolite research: archaeological and paleoenvironmental potentials. Archaeol Anthropol Sci 13:15. https://doi.org/10.1007/s12520-020-01242-8

Blong JC, Whelton HL, van Asperen EN, Bull ID, Shillito L-M (2023) Sequential biomolecular, macrofossil, and microfossil extraction from coprolites for reconstructing past behavior and environments. Front Ecol Evol 11:1131294. https://doi.org/10.3389/fevo.2023.1131294

Bouchet F, Guidon N, Dittmar K, Harter S, Ferreira LF, Chaves SM, Reinhard K, Araújo A (2003) Parasite remains in archaeological sites. Mem Inst Oswaldo Cruz 98(Suppl 1):47–52. https://doi.org/10.1590/s0074-02762003000900009

Brown S, Douka K, Collins MJ, Richter KK (2021) On the standardization of ZooMS nomenclature. J Proteomics 235:104041. https://doi.org/10.1016/j.jprot.2020.104041

Buckley M, Collins M, Thomas-Oates J, Wilson JC (2009) Species identification by analysis of bone collagen using matrix-assisted laser desorption/ionisation time-of-flight mass spectrometry. Rapid Commun Mass Spectrom 23:3843–3854. https://doi.org/10.1002/rcm.4316

Buckley M, Whitcher Kansa S, Howard S, Campbell S, Thomas-Oates J, Collins M (2010) Distinguishing between archaeological sheep and goat bones using a single collagen peptide. J Archaeol Sci 37:13–20. https://doi.org/10.1016/j.jas.2009.08.020

Bulatović J, Marković N (2013) Animal remains from medieval fortress Gradina-Trešnjevica near Ivanjica. Zb Nar Muz - Ser Arheol 21(1):292–300

Canti MG (1999) The production and preservation of faecal spherulites: animals, environment and taphonomy. J Archaeol Sci 26:251–258. https://doi.org/10.1006/jasc.1998.0322

Codlin MC, Douka K, Richter KK (2022) An application of ZooMS to identify archaeological avian fauna from Teotihuacan, Mexico. J Archaeol Sci 148:105692. https://doi.org/10.1016/j.jas.2022.105692

De Cupere B, Speleers L, Mitchell PD, Degraeve A, Meganck M, Bennion-Pedley E, Jones AK, Ledger ML, Deforce K (2022) A multidisciplinary analysis of cesspits from Late Medieval and Post-Medieval Brussels, Belgium: diet and health in the fourteenth to seventeenth centuries. Int J Hist Archaeol 26:531–572. https://doi.org/10.1007/s10761-021-00613-8

Dabney J, Knapp M, Glocke I, Gansauge M-T, Weihmann A, Nickel B, Valdiosera C, García N, Pääbo S, Arsuaga J-L, Meyer M (2013) Complete mitochondrial genome sequence of a Middle Pleistocene cave bear reconstructed from ultrashort DNA fragments. Proc Natl Acad Sci U S A 110:15758–15763. https://doi.org/10.1073/pnas.1314445110

Hunt AP, Lucas SG (2012) Descriptive terminology of coprolites and recent feces. In: Hunt AP, Milàn J, Lucas SG, Spielmann JA (eds) Vertebrate Coprolites. New Mexico Museum of Natural History and Science Bulletin 57, p53–160

Dias SRC, Cunha DES, da Silva SM, de Oliveira JB, da Silva A, Lima WDS (2013) Evaluation of parasitological and immunological aspects of acute infection by *Ancylostoma caninum* and *Ancylostoma braziliense* in mixed-breed dogs. Parasitol Res 112:2151–2157. https://doi.org/10.1007/s00436-013-3370-y

Diedrich C (2012) Typology of Ice Age spotted hyena *Crocuta crocuta spelaea* (Goldfuss, 1823) coprolite aggregate pellets from the European Late Pleistocene and their significance at dens and scavenging sites. N M Mus Nat Hist Sci Bull 57:369–377

Dufour B, Le Bailly M (2025) Paléoparasitologie et logis animal: utiliser les parasites intestinaux pour renseigner la présence animale et l'organisation des sites. Archéol Soc Environ 6(1):148–156. https://doi.org/10.21494/ISTE.OP.2025.1385

Eda M, Morimoto M, Mizuta T, Inoué T (2020) ZooMS for birds: discrimination of Japanese archaeological chickens and indigenous pheasants using collagen peptide fingerprinting. J Archaeol Sci Rep 34:102635. https://doi.org/10.1016/j.jasrep.2020.102635

Eskew WH, Ledger ML, Lloyd A, Pyles G, Gosker J, Mitchell PD (2019) Intestinal parasites in an Ottoman period latrine from Acre (Israel) dating to the early 1800s CE. Korean J Parasitol 57:575–580. https://doi.org/10.3347/kjp.2019.57.6.575

Brönnimann D, Pümpin C, Ismail-Meyer K, Rentzel P, Égüez N (2017) Excrements of omnivores and carnivores. In: Courty CN, Goldberg A, Macphail P (eds) Archaeological Soil and Sediment Micromorphology, p 67–81. https://doi.org/10.1002/9781118941065.ch7

Fellows Yates JA, Lamnidis TC, Borry M, Andrades Valtueña A, Fagernäs Z, Clayton S, Garcia MU, Neukamm J, Peltzer A (2021) Reproducible, portable, and efficient ancient genome reconstruction with nf-core/eager. PeerJ 9:e10947. https://doi.org/10.7717/peerj.10947

Gansauge M-T, Aximu-Petri A, Nagel S, Meyer M (2020) Manual and automated preparation of single-stranded DNA libraries for the sequencing of DNA from ancient biological remains and other sources of highly degraded DNA. Nat Protoc 15:2279–2300. https://doi.org/10.1038/s41596-020-0386-5

Garcia LS (2016) Diagnostic medical parasitology, 6th edn. ASM Press, Washington, DC

van Geel B, Coope GR, van der Hammen T (1989) Palaeoecology and stratigraphy of the Late-glacial type section at Usselo (The Netherlands). Rev Palaeobot Palynol 60:25–129. https://doi.org/10.1016/0034-6667(89)90072-9

Graff A, Bennion-Pedley E, Jones AK, Ledger ML, Deforce K, Degraeve A, Byl S, Mitchell PD (2020) A comparative study of parasites in three latrines from Medieval and Renaissance Brussels, Belgium (14th–17th centuries). Comp Parasitol 147:1443–1451. https://doi.org/10.1017/S0031182020001298

Hagan RW, Hofman CA, Hübner A, Reinhard K, Schnorr S, Lewis CM Jr, Sankaranarayanan K, Warinner CG (2020) Comparison of extraction methods for recovering ancient microbial DNA from paleofeces. Am J Phys Anthropol 171:275–284. https://doi.org/10.1002/ajpa.23978

Horwitz L, Goldberg KP (1989) A study of Pleistocene and Holocene hyaena coprolites. J Archaeol Sci 16:71–94. https://doi.org/10.1016/0305-4403(89)90057-5

Ledger ML, Anastasiou E, Shillito L-M, Mackay H, Bull ID, Haddow SD, Knüsel CJ, Mitchell PD (2019a) Parasite infection at the early farming community of Çatalhöyük. Antiquity 93:573–587. https://doi.org/10.15184/aqy.2019.61

Ledger ML, Grimshaw E, Fairey M, Whelton HL, Bull ID, Ballantyne R, Knight M, Mitchell PD (2019b) Intestinal parasites at the Late Bronze Age settlement of Must Farm, in the fens of East Anglia, UK (9th century B.C.E.). Parasitology 146:1583–1594. https://doi.org/10.1017/S0031182019001021

Ledger ML, Mitchell PD (2022) Tracing zoonotic parasite infections throughout human evolution. Int J Osteoarchaeol 32(3):553–564. https://doi.org/10.1002/oa.2786

Ledger ML, Murchie TJ, Dickson Z, Kuch M, Haddow SD, Knüsel CJ, Stein GJ, Parker Pearson M, Ballantyne R, Knight M, Deforce K, Carroll M, Rice C, Franconi T, Šarkić N, Redžič S, Rowan E, Cahill N, Poblome J, Palma MF, Brückner H, Mitchell PD, Poinar H (2025) Sedimentary ancient DNA as part of a multimethod paleoparasitology approach reveals temporal trends in human parasitic burden in the Roman period. PLoS Negl Trop Dis 19(6):e0013135. https://doi.org/10.1371/journal.pntd.0013135

Leles D, Gardner SL, Reinhard K, Iniguez AM, Araujo A, Ferreira LF (2012) Are *Ascaris lumbricoides* and *Ascaris suum* a single species? Parasit Vectors 5:42. https://doi.org/10.1186/1756-3305-5-42

Liu G, Zhang S, Zhao X, Li C, Gong M (2021) Advances and limitations of next generation sequencing in animal diet analysis. Genes 12(12):1854. https://doi.org/10.3390/genes12121854

Liu GH, Wu CY, Son HQ, Wei SJ, Xu MJ, Lin RQ, Zha GH, Huang SY, Zhu XQ (2012) Comparative analyses of the complete mitochondrial genomes of *Ascaris lumbricoides* and *Ascaris suum* from humans and pigs. Gene 492:110–116. https://doi.org/10.1016/j.gene.2011.10.043

Maicher C, Maigrot Y, Mazurkevich A, Dolbunova E, Le Bailly M (2021) First contribution of paleoparasitology to the study of coprolites from the Neolithic site Serteya II (NW Russia). J Archaeol Sci Rep 38:103093. https://doi.org/10.1016/j.jasrep.2021.103093

Marković N, Bulić D, Bulatović J, Marić M (2023) Relative and absolute chronology of the medieval fortress Gradina-Radaljevo near Ivanjica. J Serb Archaeol Soc 39:146–166

Mehlhorn H (2016) Animal parasites: diagnosis, treatment, prevention. Springer

Mentzer SM (2018) Micromorphological analyses of anthropogenic materials and insights into tell formation processes at Aşıklı Höyük, 2008–2012 field seasons. In: Özbaşaran M, Atakuman GD, Özkaya MB (eds) *The Early Settlement of Aşıklı Höyük: Essays in Honor of Ufuk Esin*, p 105–128

Michelsen C, Pedersen MW, Fernandez-Guerra A, Zhao L, Petersen TC, Korneliussen TS (2022) metaDMG – a fast and accurate ancient DNA damage toolkit for metagenomic data. bioRxiv. https://doi.org/10.1101/2022.12.06.519264

Goldberg P (2000) Micromorphological aspects of site formation at Keatley Creek. In: Hayden B (ed) The Ancient Past of Keatley Creek, Vol. 1, p 81–94

Mitchell PD (2015) Human parasites in medieval Europe: lifestyle, sanitation and medical treatment. Adv Parasitol 90:389–420. https://doi.org/10.1016/bs.apar.2015.05.001

Mitchell PD, Anastasiou E, Whelton HL, Bull ID, Parker Pearson M, Shillito L-M (2022) Intestinal parasites in the Neolithic population who built Stonehenge (Durrington Walls, 2500 BCE). Parasitology 149:1027–1033. https://doi.org/10.1017/S0031182022000476

Nicosia C, Canti MG (2017) Chaff. In: Nicosia C, Stoops G (eds) Archaeological Soil and Sediment Micromorphology. John Wiley & Sons, p 137–139. https://doi.org/10.1002/9781118941065

Nijsse R, Ploeger HW, Wagenaar JA, Mughini-Gras L (2015) *Toxocara canis* in household dogs: prevalence, risk factors and owners' attitude towards deworming. Parasitol Res 114:561–569. https://doi.org/10.1007/s00436-014-4218-9

Pümpin C, Le Bailly M, Pichler S (2017) Ova of intestinal parasites. In: Courty CN, Goldberg A, Macphail P (eds) Archaeological Soil and Sediment Micromorphology, pp 91–97. https://doi.org/10.1002/9781118941065.ch9

Pals JP, van Geel B, Delfos A (1980) Paleoecological studies in the Klokkeweel bog near Hoogkarspel (Noord Holland). Rev Palaeobot Palynol 30:371–418

Pedersen MW, Ruter A, Schweger C, Friebe H, Staff RA, Kjeldsen KK, Mendoza MLZ, Beaudoin AB, Zutter C, Larsen NK, Potter BA, Nielsen R, Rainville RA, Orlando L, Meltzer DJ, Kjær KH, Willerslev E (2016) Postglacial viability and colonization in North America's ice-free corridor. Nature 537:45–49. https://doi.org/10.1038/nature19085

Pichler SL, Pümpin C, Brönnimann D, Rentzel P (2014) Life in the proto-urban style: the identification of parasite eggs in micromorphological thin sections from the Basel-Gasfabrik Late Iron Age settlement, Switzerland. J Archaeol Sci 43:55–65. https://doi.org/10.1016/j.jas.2013.12.002

Rabinow S, Wang T, Wilson RJA, Mitchell PD (2022) Using parasite analysis to identify ancient chamber pots: an example of the fifth century CE from Gerace, Sicily, Italy. J Archaeol Sci Rep 42:103349. https://doi.org/10.1016/j.jasrep.2022.103349

Rabinow S, Wang T, van Oosten R, Meijer Y, Mitchell PD (2024) Intestinal parasite infection and sanitation in medieval Leiden, the Low Countries. Antiquity 98(400):1006–1022. https://doi.org/10.15184/aqy.2024.72

Reinhard KJ, Confalonieri UE, Herrmann B, Ferreira LF, de Araujo AJG (1986) Recovery of parasite remains from coprolites and latrines: aspects of paleoparasitological technique. Homo 37(4):217–239

Reinhard K, Camacho M, Geyer B, Hayek S, Horn C, Otterson K, Russ J (2019) Imaging coprolite taphonomy and preservation. Archaeol Anthropol Sci 11:6017–6035. https://doi.org/10.1007/s12520-019-00946-w

Roberts LS, Janovy J Jr (2008) Foundations of parasitology, 8th edn. McGraw Hill, New York

Romaniuk A, Panciroli E, Buckley M, Chowdhury MP, Willars C, Herman JS, Troalen LG, Shepherd AN, Clarke DV, Sheridan A, van Dongen BE, Butler IB, Bendrey R (2020) Combined visual and biochemical analyses confirm depositor and diet for Neolithic coprolites from Skara Brae. Archaeol Anthropol Sci 12:1–15. https://doi.org/10.1007/s12520-020-01225-9

Scott L (1987) Pollen analysis of hyena coprolites and sediments from Equus Cave, Taung, southern Kalahari (South Africa). Quat Res 28:144–156. https://doi.org/10.1016/0033-5894(87)90039-1

Shalaby HA, Abdel-Shafy S, Derbala AA (2010) The role of dogs in transmission of *Ascaris lumbricoides* for humans. Parasitol Res 106:1021–1026. https://doi.org/10.1007/s00436-010-1755-8

Shillito L-M, Blong JC, Green EJ, van Asperen EN (2020a) The what, how and why of archaeological coprolite analysis. Earth Sci Rev 207:103196. https://doi.org/10.1016/j.earscirev.2020.103196

Shillito L-M, Whelton HL, Blong JC, Jenkins DL, Connolly TJ, Bull ID (2020b) Pre-Clovis occupation of the Americas identified by human faecal biomarkers in coprolites from Paisley Caves, Oregon. Sci Adv 6:eaba6404. https://doi.org/10.1126/sciadv.aba6404

Slepchenko SM, Khrustalev AV, Ivanov SN, Titova IV, Kasparov AK, Chasnyk VG, Pavlova EY, Pitulko VV (2025a) Early history of parasitic diseases in northern dogs revealed by dog paleofeces from the 9000-year-old frozen Zhokhov site in the New Siberian Islands of East Siberian Arctic. J Archaeol Sci 163:106337. https://doi.org/10.1016/j.jas.2025.106337

Stoops G (2021) Guidelines for analysis and description of soil and regolith thin sections, 2nd ed. John Wiley & Sons, Hoboken

Strohalm M, Hassman M, Kosata B, Kodícek M (2008) mMass data miner: an open source alternative for mass spectrometric data analysis. Rapid Commun Mass Spectrom 22:905–908. https://doi.org/10.1002/rcm.3444

Stucki K, Dal Cero M, Vogl CR, Ivemeyer S, Meier B, Maeschli A, Hamburger M, Walkenhorst M (2019) Ethnoveterinary contemporary knowledge of farmers in pre-alpine and alpine regions of the Swiss cantons of Bern and Lucerne compared to ancient and recent literature – is there a tradition? J Ethnopharmacol 234:225–244. https://doi.org/10.1016/j.jep.2018.12.022

Tolar T, Galik A (2019) A study of dog coprolite from Late Neolithic pile-dwelling site in Slovenia. Archaeol Discov 7:20–29. https://doi.org/10.4236/ad.2019.71002

Tolar T, Galik A, Le Bailly M, Dufour B, Caf N, Toškan B, Bužan E, Zver L, Janžekovič F, Velušček A (2021) Multi-proxy analysis of waterlogged preserved Late Neolithic canine excrements. Veg Hist Archaeobot 30:107–118. https://doi.org/10.1007/s00334-020-00805-y

Tripp M, Wiemann J, Brocks J, Mayer P, Schwark L, Grice K (2022) Fossil biomarkers and biosignatures preserved in coprolites reveal carnivorous diets in the Carboniferous Mazon Creek ecosystem. Biology 11(9):1289. https://doi.org/10.3390/biology11091289

Welker F, Hajdinjak M, Talamo S, Jaouen K, Dannemann M, David F, Julien M, Meyer M, Kelso J, Barnes I, Brace S, Kamminga P, Fischer R, Kessler BM, Stewart JR, Pääbo S, Collins MJ, Hublin J-J (2016) Palaeoproteomic evidence identifies archaic hominins associated with the Châtelperronian at the Grotte du Renne. Proc Natl Acad Sci U S A 113:11162–11167. https://doi.org/10.1073/pnas.1605834113

Witt KE, Yarlagadda K, Allen JM, Bader AC, Simon ML, Kuehn SR, Swanson KS, Cross T-WL, Hedman KM, Ambrose SH, Malhi RS (2021) Integrative analysis of DNA, macroscopic remains and stable isotopes of dog coprolites to reconstruct community diet. Sci Rep 11:3113. https://doi.org/10.1038/s41598-021-82362-6

Brown S (2021) Identifying ZooMS spectra (mammals) using mMass v1. https://doi.org/10.17504/protocols.io.bzscp6aw